JAERI-M
87-178

ATTAINMENT OF HIGH ION TEMPERATURE PLASMAS IN JT-60 AND ANALYSIS ON THEIR TRANSPORT CHARACTERISTICS

November 1987

Nobuyuki HOSOGANE, Katsuhiro SHIMIZU, Hiroshi SHIRAI
Yoshinori KUSAMA, Kenji TOBITA, Masahiro NEMOTO
Akira SAKASAI, Yoshihiko KOIDE, Keisuke NAGASHIMA
Hidetoshi YOSHIDA and JT-60 Team

日本原子力研究所
Japan Atomic Energy Research Institute

JAERI-Mレポートは，日本原子力研究所が不定期に公刊している研究報告書です。
入手の問合わせは，日本原子力研究所技術情報部情報資料課（〒319-11茨城県那珂郡東海村）あて，お申しこしください。なお，このほかに財団法人原子力弘済会資料センター（〒319-11 茨城県那珂郡東海村日本原子力研究所内）で複写による実費頒布をおこなっております。

JAERI-M reports are issued irregularly.
Inquiries about availability of the reports should be addressed to Information Division Department of Technical Information, Japan Atomic Energy Research Institute, Tokai-mura, Naka-gun, Ibaraki-ken 319-11, Japan.

編集兼発行　日本原子力研究所
印　　刷　いばらき印刷㈱

JAERI-M 87-178

Attainment of High Ion Temperature Plasmas in JT-60 and Analysis on Their Transport Characteristics

Nobuyuki HOSOGANE, Katsuhiro SHIMIZU, Hiroshi SHIRAI
Yoshinori KUSAMA, Kenji TOBITA, Masahiro NEMOTO
Akira SAKASAI, Yoshihiko KOIDE, Keisuke NAGASHIMA
Hidetoshi YOSHIDA and JT-60 Team*

Department of Large Tokamak Research
Naka Fusion Research Establishment
Japan Atomic Energy Research Institute
Naka-machi, Naka-gun, Ibaraki-ken

(Received October 7, 1987)

High ion temperatures above 10 keV were obtained in JT-60 limited plasmas by the high power neutral beam heating ($H^0 \rightarrow H^+$), which is much higher than the maximum value, 6.5 keV, obtained in JT-60 diverted plasmas. The experiment was performed in the parameter region of I_p = 1-2 MA, $\bar{n}_e|_{\text{before heating}} = 0.7\text{-}1.5\times10^{19}$ m^{-3}, $\bar{n}_e|_{\text{end of heating}} = 2.5\text{-}4.1\times10^{19}$ m^{-3} and P_{NB}^{inj} = 19-21.8 MW. Z_{eff} of the limited plasmas were high, 4-7, compared with those of the diverted plasmas, 1-2. According to the transport analysis on the difference in ion temperature between these plasmas with different Z_{eff}, it is found that (1) because of increase in deposition power to electron, P_{be}, with Z_{eff}, high Z_{eff} is effective to raising electron temperature, and (2) since the equipartition loss is reduced by increase in electron temperature, high ion temperature is obtained in the limited plasmas with high Z_{eff}.

Keywords: JT-60, High Ion Temperature, Neutral Beam Heating, Limited Plasmas, Transport Analysis, High Z_{eff}

* T.ABE, H.AIKAWA, N.AKAOKA, H.AKASAKA, M.AKIBA, N.AKINO, T.AKIYAMA, T.ANDO
K.ANNOH, N.AOYAGI, T.ARAI, K.ARAKAWA, M.ARAKI, K.ARIMOTO, M.AZUMI, S.CHIBA
M.DAIRAKU, N.EBISWA, T.FUJII, T.FUKUDA, H.FURUKAWA, K.HAMAMATSU, M.HARA
K.HARAGUCHI, H.HIRATSUKA, T.HIRAYAMA, S.HIROKI, K.HIRUTA, M.HONDA
H.HORIIKE, R.HOSODA, N.HOSOGANE, Y.IIDA, T.IIJIMA, K.IKEDA, Y.IKEDA
T.IMAI, T.INOUE., N.ISAJI, M.ISAKA, S.ISHIDA, N.ITIGE, T.ITO, Y.ITO
A.KAMINAGA, T.KATO, M.KAWAI, Y.KAWAMATA, K.KAWASAKI, K. KIKUCHI, M.KIKUCHI
H.KIMURA, T.KIMURA, H.KISHIMOTO, K.KITAHARA, S.KITAMURA, A.KITSUNEZAKI
K.KIYONO, N.KOBAYASHI, K.KODAMA, Y.KOIDE, T.KOIKE, M.KOMATA, I.KONDO
S.KONOSHIMA, H.KUBO, S.KUNIEDA, K.KURIHARA, M.KURIYAMA, T.KURODA, M.KUSAKA
Y.KUSAMA, S.MAEBARA, K.MAENO, S.MATSUDA, M.MATSUKAWA, T.MATSUKAWA
M.MATSUOKA, N.MIYA, K.MIYATI, Y.MIYO, K.MIZUHASHI, M.MIZUNO, R.MURAI
Y.MURAKAMI, M.MUTO, M.NAGAMI, A.NAGASHIMA, K.NAGASHIMA, T.NAGASHIMA
S.NAGAYA, H.NAKAMURA, Y.NAKAMURA, M.NEMOTO, Y.NEYATANI, H.NINOMIYA
N.NISHINO*4, T.NISHITANI, H.NOMATA, K.OBARA, N.OGIWARA, T.OHGA, Y.OHARA
K.OHASA, H.OOHARA, T.OHSHIMA, M.OHKUBO, K.OHTA, M.OHTA, M.OHTAKA
Y.OHUCHI, A.OIKAWA, H.OKUMURA, Y.OKUMURA, K.OMORI, S.OMORI, Y.OMORI
T.OZEKI, A.SAKASAI, S.SAKATA, M.SATOU, M.SAIGUSA, K.SAKAMOTO, M.SAWAHATA
M.SEIMIYA, M.SEKI, S.SEKI, K.SHIBANUMA, R.SHIMADA, K.SHIMIZU, M.SHIMIZU
Y.SHIMOMURA, S.SHINOZAKI, H.SHIRAI, H.SHIRAKATA, M.SHITOMI, K.SUGANUMA
T.SUGIE, T.SUGIYAMA, H.SUNAOSHI, K.SUZUKI, M.SUZUKI*4, M.SUZUKI, N.SUZUKI
S.SUZUKI, Y.SUZUKI, M.TAKAHASHI, S.TAKAHASHI, T.TAKAHASHI, M.TAKASAKI
H.TAKATSU, H.TAKEUCHI, A.TAKESHITA, S.TAMURA, S.TANAKA, T.TANAKA, K.TANI
M.TERAKADO, T.TERAKADO, K.TOBITA, T.TOKUTAKE, T.TOTSUKA, N.TOYOSHIMA
F.TSUDA, T.TSUGITA, S.TSUJI, Y.TSUKAHARA, M.TSUNEOKA, K.UEHARA
M.UMEHARA, Y.URAMOTO, H.USAMI, K.USHIGUSA, K.USUI, J.YAGYU, T.YAMAGUCHI
M.YAMAMOTO, O.YAMASHITA, Y.YAMASHITA, K.YANO, T.YASUKAWA, K.YOKOKURA
H.YOKOMIZO, K.YOSHIKAWA, M.YOSHIKAWA, H.YOSHIDA, Y.YOSHINARI, R.YOSHINO
K.YOSHIYUKI*4, I.YONEKAWA, T.YONEDA, K.WATANABE, M.BELL*1, R.BICKERTON*2
W.ENGELHARDT*2, E.KÄLLNE*2, J.KÄLLNE*2, J.STEVENS*1, Y.TAKASE*3
P.THOMAS*2

*1 Princeton Plasma Physics Laboratory, USA
*2 JET Joint Undertaking, EC
*3 Massachusetts Institute of Technology, USA
*4 Contract Researcher

JAERI－M　87－178

JT－60における高イオン温度プラズマの達成及びその輸送特性の解析

日本原子力研究所那珂研究所臨界プラズマ研究部
細金延幸・清水勝宏・白井　浩・草間義紀
飛田健次・根本正博・逆井　章・小出芳彦
永島圭介・吉田英俊・JT－60チーム※

（1987年10月7日受理）

JT－60のリミタプラズマにおいて高パワー中性粒子ビーム加熱（$H^0 \rightarrow H^+$）によって，10 keV以上の高イオン温度が得られた。この値は，JT－60ダイバータプラズマで得られた最大イオン温度6.5 keVより，非常に大きなものである。この実験は，$I_p = 1 - 2$ MA，$\bar{n}_e$（加熱前）$= 0.7 - 1.5 \times 10^{19} m^{-3}$，$\bar{n}_e$（加熱直後）$= 2.5 - 4.1 \times 10^{19} m^{-3}$ で行われた。このリミタプラズマのZ_{eff}は，ダイバータプラズマのZ_{eff}，1～2，と比べると非常に高く，4～7であった。Z_{eff}が異なるこれらのプラズマのイオン温度に対する輸送解析の結果，次のことがわかった。

(1) Z_{eff}が大きくなると，電子への入力パワーP_{bc}が増大するため，高Z_{eff}であることは，電子温度を上げることに効果的である。

(2) 電子温度が上昇すると，エネルギー緩和損失が減少するので，高Z_{eff}のリミタプラズマでは，高イオン温度が得られる。

那珂研究所：〒311－02 茨城県那珂郡那珂町大字向山801－1

* 相川　裕史・青柳　哲雄・赤岡　伸雄・赤坂　博美・秋野　昇・秋場　真人・秋山　隆
安積　正史・阿部　哲也・新井　貴・荒川喜代次・荒木　政則・有本　公子・安東　俊郎
安納　勝人・飯島　勉・飯田　幸生・池田　幸治・池田　佳隆・井坂　正義・伊佐治信明
石田　真一・市毛　尚志・伊藤　孝雄・伊藤　康治・井上多加志・今井　剛・上原　和也
宇佐美広次・牛草　健吉・薄井　勝富・梅原　昌敏・浦本　保幸・海老沢　昇・及川　晃
大麻　和美・大内　豊・大賀　徳道・大久保　実・大島　貴幸・太田　和也・太田　充
大高　光夫・大原比呂志・大森憲一郎・大森　俊造・大森　栄和・荻原　徳男・奥村　裕司
奥村　義和・小関　隆久・小原建治郎・小原　祥裕・加藤　次男・神永　敦嗣・河合視己人
川崎　幸三・川俣　陽一・菊池　勝美・菊池　満・岸本　浩・北原　勝美・北村　繁
孤崎　晶雄・木村　豊秋・木村　晴行・清野　公広・日下　誠・草間　義紀・国枝　俊介
久保　博孝・栗原　研一・栗山　正明・黒田　猛・小池　常之・小出　芳彦・児玉　幸三
木島　滋・小林　則幸・小又　将夫・近藤　育朗・三枝　幹雄・逆井　章・坂田　信也
坂本　慶司・佐藤　正泰・沢畠　正之・郡　守正・篠崎　信一・紫沼　清・嶋田　隆一
清水　勝宏・清水　正亜・下村　安夫・白井　浩・白形　弘文・菅沼　和明・杉江　達夫
杉山　隆・鈴木　貞明・鈴木　國弘・鈴木　紀男・鈴木　正信[*4]・鈴木　道雄・鈴木　康夫
砂押　秀則・清宮　宗孝・関　正美・関　省吾・高崎　学・高津　英幸・高橋　春次
高橋虎之助・高橋　実・竹内　浩・竹下　明・田中　茂・田中竹次郎・谷　啓二
田村　早苗・大楽　正幸・千葉　真一・塚原　美光・次田　友宜・辻　俊二・津田　文男
恒岡まさき・寺門　恒久・寺門　正之・徳竹　利国・戸塚　俊之・飛田　健次・豊島　昇
中村　博雄・中村　幸治・長島　章・永島　圭介・永島　孝・永谷　進・永見　正幸
西谷　健夫・西野　信博[*4]・二宮　博正・根本　正博・閨谷　譲・野亦　英幸・濱松　清隆
原　誠・原口　和三・平塚　一・平山　俊雄・蛭田　和治・廣木　成治・福田　武司
藤井　常幸・古川　弘・細金　延幸・細田隆二郎・堀池　寛・本田　正男・前野　勝樹
前原　直・松岡　守・松川　達哉・松川　誠・松田慎三郎・水野　誠・水橋　清
宮　直之・宮地　謙吾・三代　康彦・武藤　貢・村井　隆一・村上　義夫・柳生　純一
安川　享・矢野　勝久・山下　修・山下　幸彦・山口　健・山本　正弘・横倉　賢治
横溝　英明・吉川　和伸・吉川　允二・吉田　英俊・吉成　洋治・芳野　隆治・吉行　健[*4]
米川　出・米田　毅・渡邊　和弘・M. Bell[*1]・R. Bickerton[*2]・W. Engelhardt[*2]
E. Källne[*2]　J. Källne[*2]・J. Stevens[*1]・Y. Takase[*3]・P. Thomas[*2]

*1 Princeton Plasma Physics Laboratory, U.S.A.
*2 JET Joint Undertaking, EC
*3 Massachusetts Institute of Technology, U.S.A.
*4 外来研究員

Contents

目　　次

1. Introduction

Attainment of high ion temperature plasmas with order of 10 keV is one of most important issues in the nuclear fusion program. Recent experiments in large tokamaks, JET and TFTR, have demonstrated that such fusion grade plasmas with high ion temperature above 10 keV can be obtained with high power neutral beam heating in the low electron density regime (12.5 keV in JET and 20 keV in TFTR) [1,2].

JT-60 is also a large tokamak with a compact poloidal diverter, objecting the break-even plasma with high power auxiliary heating systems[3]. In JT-60, neutral beam heating experiment with power up to 20 MW started in August, 1986. Confinement characteristics have been studied mainly in the divertor configuration, and the L-mode type scaling of energy confinement time has been obtained (τ_E=100 msec at P_{abs}=20 MW for 2 MA plasmas). In spite of high power neutral beam heating, ion and electron temperatures obtained in this experiment were 6.5 keV and 4 keV even in the low density of 2.5×10^{19} m^{-3}.

Recently, high ion temperature above 10 keV has been also attained in JT-60 by injecting high power neutral beam of 20 MW into the limited plasmas with low density of 0.7×10^{19} m^{-3}. The experiment was performed in the region of I_p=1-2 MA, $\bar{n}_e$=0.7-1.5×10^{19} m^{-3} before the heating and $\bar{n}_e$=2.5-4.1×10^{19} m^{-3} at the end of the heating. Compared with the results in the experiments on the diverted plasmas, ion and electron temperatures obtained in this experiment are higher as a whole. Because of the low electron density discharges, Z_{eff} of the limited plasmas are much higher than those of the diverted plasmas, which seems to be a "key" to the attainment of high ion temperature in this experiment. Hence, taking account of the effect of impurity ions, the transport characteristics of both plasmas are investigated on the difference in ion temperature by using the one dimensional time independent transport analysis code.

In section 2, the experimental arrangement of JT-60 is briefly described. In section 3, a typical discharge in which high ion temperature was obtained is presented. In section 4, characteristics of the limited and the diverted plasmas are compared each other. In section 5, the transport analysises on both plasmas are described, and the cause of the difference in ion temperature is discussed. Section 6 is discussion and conclusion.

2. Experimental arrangement

The cross-sectional view of JT-60 and a typical limited plasma configuration in this experiment are shown in Fig. 1. The major radius of the vacuum vessel is 3.04 m and the minor radius is 0.93 m. The molybdenum limiters and the molybdenum or inconnel armor coated with TiC are used as the first wall. The detailed description of the JT-60 tokamak is given in Ref.[3].

Fourteen units of the neutral beam injectors (NBI) are arranged at different seven toroidal sections. Each of the cross-sectional view is same as shown in Fig. 1. Each beam line is almost perpendicular (±78 degrees) to the toroidal direction, and passes through the point slightly off the axis of the vessel, R=2.84 m, on the midplane. Because of the off-axis injection, the deposition of the neutral beam power has a peak around the position of r=0.25 m from the magnetic axis for both the limited and diverted plasmas. The ratio of co- and couter-injection is 8:6. Hydrogen beam with energy of 70-75 keV and power of 16-22 MW was injected in this experiment.

The arrangement of key diagnostics used here is also shown in Fig. 1. The electron temperature is measured by a six channel Thomson scattering system. The ion temperature is measured by the doppler braodening of titanium emission line, TiXXI and TiXXII. Especially, the measurement of central ion temperature, $T_i(0)$, is conducted by the spectroscopy of forward scattering of helium beam with energy of 190 keV which passes through the center of the vessel. As the pulse length of the helium beam is 100 msec, the measurement was conducted at the same time as the Thomson scattering measurement. The electron density is measured by a three channel CO_2 laser interferometer. Z_{eff} is measured by the spectroscopy of visible bremsstrahlung and the soft X-ray spectroscopy. The radiation is measured by a fifteen channel bolometer.

3. Typical limiter discharge with high ion temperature

In Fig. 2, typical waveforms are shown of the limited plasma discharge with 18.8 MW neutral beam heating in which high ion temperature above 10 keV was obtained. The plasma current is 1 MA.

2. Experimental arrangement

The cross-sectional view of JT-60 and a typical limited plasma configuration in this experiment are shown in Fig. 1. The major radius of the vacuum vessel is 3.04 m and the minor radius is 0.93 m. The molybdenum limiters and the molybdenum or inconnel armor coated with TiC are used as the first wall. The detailed description of the JT-60 tokamak is given in Ref.[3].

Fourteen units of the neutral beam injectors (NBI) are arranged at different seven toroidal sections. Each of the cross-sectional view is same as shown in Fig. 1. Each beam line is almost perpendicular (±78 degrees) to the toroidal direction, and passes through the point slightly off the axis of the vessel, R=2.84 m, on the midplane. Because of the off-axis injection, the deposition of the neutral beam power has a peak around the position of r=0.25 m from the magnetic axis for both the limited and diverted plasmas. The ratio of co- and couter-injection is 8:6. Hydrogen beam with energy of 70-75 keV and power of 16-22 MW was injected in this experiment.

The arrangement of key diagnostics used here is also shown in Fig. 1. The electron temperature is measured by a six channel Thomson scattering system. The ion temperature is measured by the doppler braodening of titanium emission line, TiXXI and TiXXII. Especially, the measurement of central ion temperature, $T_i(0)$, is conducted by the spectroscopy of forward scattering of helium beam with energy of 190 keV which passes through the center of the vessel. As the pulse length of the helium beam is 100 msec, the measurement was conducted at the same time as the Thomson scattering measurement. The electron density is measured by a three channel CO_2 laser interferometer. Z_{eff} is measured by the spectroscopy of visible bremsstrahlung and the soft X-ray spectroscopy. The radiation is measured by a fifteen channel bolometer.

3. Typical limiter discharge with high ion temperature

In Fig. 2, typical waveforms are shown of the limited plasma discharge with 18.8 MW neutral beam heating in which high ion temperature above 10 keV was obtained. The plasma current is 1 MA.

The ohmic plasma with low electron density of 0.7×10^{19} m^{-3} is produced without any additional gas puff after the break down. The electron and ion temperatures just before the neutral beam heating are 4.8 keV and 3 keV, respectively. The hydrogen neutral beam with energy of 70 keV is injected at 6.5 sec. The electron density rises up to 2.5×10^{19} m^{-3} at 7.0 sec, and almost saturates at 0.5 sec after the injection of the neutral beam. The electron temperature measured by the doppler broadening of TiXXII, T_i^{TiXXII}, rises up to 8.3±1.5 keV. While, the ion temperature measured by the forward scattering of helium beam, T_i^{AB}, is 11±2 keV. Since the latter temperature is determined by the spectrum of the helium beam scattered around the plasma center, it is considered a central ion temperature. The radiation loss during the neutral beam heating is about 10 MW, assuming the toroidal symmetry of the radiation. Z_{eff} during the heating is 4-7.

4. Characteristics of the limiter discharges and the divertor discharges

Figure 3 shows the absorbed power dependence of ion and electron temperatures obtained in the neutral beam heating of the limited and diverted plasmas. Also, the electron density dependence of them is shown in Fig. 4. Here, it should be noted that ion temperatures measured by the doppler broadening of TiXXI or TiXXII, T_i^{TiXXII}, are lower than central ones, but can be used to see tendencies of their parameter dependences. The comparison of absolute values of central ion temperatures should be made among ones determined by the forward scattering measurement of helium beam. As for the limited plasmas, central temperatures above 10 keV are obtained with absorbed power of 16.5-17.5 MW and electron density of $2.5\text{-}2.7\times10^{19}$ m^{-3}. While, the maximum central ion temperature of diverted plasmas is 6.5±0.8 keV. This value may be corrected by using the absorbed power dependence of ion temperature, T_i^{TiXXI}, but will be still much smaller than central temperatures of the limited plasmas.

As shown in Figs. 3 and 4, the electron temperature does not increase so much with absorbed power and electron density for both the limited and the diverted plasmas. In the diverted discharges with electron density of $2\text{-}4\times10^{19}$ m^{-3}, electron temperatures are 3-4 keV.

The ohmic plasma with low electron density of 0.7×10^{19} m^{-3} is produced without any additional gas puff after the break down. The electron and ion temperatures just before the neutral beam heating are 4.8 keV and 3 keV, respectively. The hydrogen neutral beam with energy of 70 keV is injected at 6.5 sec. The electron density rises up to 2.5×10^{19} m^{-3} at 7.0 sec, and almost saturates at 0.5 sec after the injection of the neutral beam. The electron temperature measured by the doppler broadening of TiXXII, T_i^{TiXXII}, rises up to 8.3±1.5 keV. While, the ion temperature measured by the forward scattering of helium beam, T_i^{AB}, is 11±2 keV. Since the latter temperature is determined by the spectrum of the helium beam scattered around the plasma center, it is considered a central ion temperature. The radiation loss during the neutral beam heating is about 10 MW, assuming the toroidal symmetry of the radiation. Z_{eff} during the heating is 4-7.

4. Characteristics of the limiter discharges and the divertor discharges

Figure 3 shows the absorbed power dependence of ion and electron temperatures obtained in the neutral beam heating of the limited and diverted plasmas. Also, the electron density dependence of them is shown in Fig. 4. Here, it should be noted that ion temperatures measured by the doppler broadening of TiXXI or TiXXII, T_i^{TiXXII}, are lower than central ones, but can be used to see tendencies of their parameter dependences. The comparison of absolute values of central ion temperatures should be made among ones determined by the forward scattering measurement of helium beam. As for the limited plasmas, central temperatures above 10 keV are obtained with absorbed power of 16.5-17.5 MW and electron density of $2.5\text{-}2.7\times10^{19}$ m^{-3}. While, the maximum central ion temperature of diverted plasmas is 6.5±0.8 keV. This value may be corrected by using the absorbed power dependence of ion temperature, T_i^{TiXXI}, but will be still much smaller than central temperatures of the limited plasmas.

As shown in Figs. 3 and 4, the electron temperature does not increase so much with absorbed power and electron density for both the limited and the diverted plasmas. In the diverted discharges with electron density of $2\text{-}4\times10^{19}$ m^{-3}, electron temperatures are 3-4 keV.

While, in the limited plasmas, higher electron temperatures of 4-5 keV are obtained in the same region of electron density.

Stored energies of the limited plasmas and the diverted plasmas are shown in Fig. 5. The stored energy is calculated as a sum of the ohmic stored energy before the neutral beam heating, $W_{OH} = 0.157 I_p^{0.86} \bar{n}_e^{0.62}$, and the incremental stored energy ΔW^*, obtained by the neutral beam heating. Here, W_{OH} is a scaling of the stored energy for ohmic plasmas in JT-60 which is derived by the transport analysis using experimental data. ΔW^* is calculated by using the increment of Shafranov lambda,

$$\Delta \Lambda = \Delta \beta_p + \Delta \frac{\ell_i}{2} \quad ,$$

assuming the variation of the internal inductance during the neutral beam heating is negligible.

In case of the 1 MA limited plasmas with ion temperature above 10 keV, the stored energies exceed those of the diverted plasmas, which tend to saturate in the region above 10 MW. The energy confinement time is 65-75 msec, which exceeds the value of the Goldston scaling, 50 msec. Here, the Goldston scaling multiplied by the square root of the mass ratio of hydrogen and deutrium, $1/\sqrt{2}$, is used as a scaling law for hydrogen plasmas. In case of the 1.5 MA and 2 MA limited plasmas, however, the stored energies are rather less than those of the diverted plasmas although the ion temperatures are still high.

Figure 6 shows the relation of Z_{eff} and electron density for both the limited and the diverted plasmas. Z_{eff} of the limited plasmas are scattered between 4 and 7. The dominant impurities are oxygen and titanium. Titanium comes from the limiters and the armor tiles coated with TiC, while the amount of carbon is small compared with that of oxygen according to the spectroscopic measurement. According to the soft X-ray spectroscopy with the pulse height analyzer, the amount of titanium is roughly estimated 0.1-0.3% with ambuguity of a factor of 2. The estimated value corresponds to the proportion of $Z_{eff} = 0.48$-1.5, assuming titanium atoms are fully ionized. The rest of Z_{eff} is considered contributed by oxygen. Hence, the proton ratio of the limited plasmas, n_p/n_e, is estimated 30-70% against Z_{eff}=4-7. On the other hand, Z_{eff} of the diverted plasmas are 1.5-2 even in the low

electron density region of $\bar{n}_e=2\times10^{19}$ m^{-3} due to the effectiveness of the divertor action.

5. Transport Analysis

The transport characteristics of the limited and the diverted plasmas is analyzed by the one dimensional time independent transport anlaysis code, LOOK/OFMC/SCOOP code[6]. The analysis is concentrated on the effect of Z_{eff} on ion temperature, electron temperature and stored energy of both plasmas.

In the LOOK code, profiles of electron denisty and electron temperature are determined as a function of magnetic flux in the equilibrium configuration by using the experimental data.

Energy and particle deposition profiles of the neutral beam is calculated by the OFMC (Orbit-Following-Monte-Carlo) code[6]. The effect of impurity ions on the deposition process is included in the calculation, assuming the uniform Z_{eff} distribution. The ionization cross-section proportional to $Z^{1.4}$ is used for the birth of fast ions[7,8]. The neutral beam power deposited to the impurity ions is added to that of the protons, and the sum is treated as a deposition power to the ions, P_{bi}. The reionization process against the charge exchange loss of fast neutral particles produced in the plasma is also included in this code.

Dependences of central ion temperatures on Z_{eff} and electron temperature are investigated by calculating the power balance equation for ions, $P_{bi}-P_{cv}-P_{cd}-P_{ie}-P_n=0$, in the SCOOP code. In the calculation, impurity ion temperature is set equal to proton temperature because the ion-ion collision time is much smaller than the electron-ion collision time. The conduction loss of the thermal ion energy, P_{cd}, is calculated with the neoclassical thermal conductivity, X_i^{CH}, given by Chang-Hinton[9]. The conduction loss of the impurity energy itself is not treated, but can be included by using an enhanced thermal conductivity, $C_i X_i^{CH}$. Here, C_i is the 'neoclassical multiplier'. The convection loss, $P_{cv}=\frac{5}{2}\Gamma T$, is calculated by using the particle flux, Γ, determined by the particle balance equation. The convection loss of the impurity energy is also

electron density region of $\bar{n}_e=2\times10^{19}$ m^{-3} due to the effectiveness of the divertor action.

5. Transport Analysis

The transport characteristics of the limited and the diverted plasmas is analyzed by the one dimensional time independent transport anlaysis code, LOOK/OFMC/SCOOP code[6]. The analysis is concentrated on the effect of Z_{eff} on ion temperature, electron temperature and stored energy of both plasmas.

In the LOOK code, profiles of electron denisty and electron temperature are determined as a function of magnetic flux in the equilibrium configuration by using the experimental data.

Energy and particle deposition profiles of the neutral beam is calculated by the OFMC (Orbit-Following-Monte-Carlo) code[6]. The effect of impurity ions on the deposition process is included in the calculation, assuming the uniform Z_{eff} distribution. The ionization cross-section proportional to $Z^{1.4}$ is used for the birth of fast ions[7,8]. The neutral beam power deposited to the impurity ions is added to that of the protons, and the sum is treated as a deposition power to the ions, P_{bi}. The reionization process against the charge exchange loss of fast neutral particles produced in the plasma is also included in this code.

Dependences of central ion temperatures on Z_{eff} and electron temperature are investigated by calculating the power balance equation for ions, $P_{bi}-P_{cv}-P_{cd}-P_{ie}-P_n=0$, in the SCOOP code. In the calculation, impurity ion temperature is set equal to proton temperature because the ion-ion collision time is much smaller than the electron-ion collision time. The conduction loss of the thermal ion energy, P_{cd}, is calculated with the neoclassical thermal conductivity, X_i^{CH}, given by Chang-Hinton[9]. The conduction loss of the impurity energy itself is not treated, but can be included by using an enhanced thermal conductivity, $C_i X_i^{CH}$. Here, C_i is the 'neoclassical multiplier'. The convection loss, $P_{cv}=\frac{5}{2}\Gamma T$, is calculated by using the particle flux, Γ, determined by the particle balance equation. The convection loss of the impurity energy is also

neglected. The equipartition loss, P_{ie}, is a sum of the proton-electron equipartition loss and the impurity-electron equipartition loss, that is, expressed as

$$P_{ie} = 3/2\ n_{eff}/\tau_{ei}(T_i - T_e) \quad .$$

Here, for purposes of convenience, the "effective number of ions",

$$n_{eff} = n_p + n_z Z^2\ m_p/m_z \quad ,$$

is defined, where n_p, n_z, m_p and m_z are the numbers of proton and impurity and the masses of them, respectively. τ_{ie} is ion-electron collision time. In the calculation for the low electron density region, the number of fast ions, n_f, becomes unnegligible compared with that of the thermal ions. In the power balance equation, the number of the thermal ions, $n_{th}(r)$, defined by the equation, $n_{th}(r) = n_p(r) - n_f(r)$, is used.

In the following transport analysis, only an effect of oxygen ions is taken into account as a dominant impurity effect. In the calculation for the limited plasmas, an effect of titanium ions which corresponds to the amount of $\Delta Z_{eff}=1$ is indirectly treated in the following way. In the SCOOP code, $Z_{eff}^{SCOOP}=Z_{eff}-1$ is used excluding the contribution of titanium. While, in the OFMC code, $Z_{eff}^{OFMC}=Z_{eff}$ is used, but the particle confinement time τ_p^{PFMC}, is reduced to $\tau_p^{OFMC} = \tau_p\ n_p/(n_p+\Delta n_p)$ because the proportion of proton, n_p/n_e, increases by the amount corresponding to $\Delta Z_{eff}=1$, Δn_p. With the reduced value of τ_p^{OFMC}, the stored energy stays at the reasonable value even at $Z_{eff}=6$ due to the increase in charge exchange loss.

Figure 7 shows the comparison of the central ion temperatures calculated in the LOOK/OFMC/SCOOP code and the ion temperatures obtained in the experiments of the limited and the diverted plasmas against the electron density of $2.5\text{-}5.7\times10^{19}$ m^{-3}. Good agreements are obtained between these ion temperatures. Here, in the calculation, $Z_{eff}=6$ is used for the limited plasmas although the values of Z_{eff} are scattered between 4 and 7 in the experiment. But, as described later, the Z_{eff}-dependence of ion temperature is week as long as the measured electron temperatures are used in the calculation, and the result does not change so much with the other value of Z_{eff}. As for the diverted

plasmas, Z_{eff}=1.5 is used. In the calculation of the conduction loss, C_i=1 is used for both plasmas. Since the conduction loss is small as described later, the difference is small between ion temperatures calculated with C_i=1 and those with C_i=3. As for the stored energies, the following relation between the calculated stored energies, W_{tot}, and the measured ones, W*, is obtained;

$$W_{tot} = 1.1W^* \pm 0.07W^* \quad .$$

Reasonable agreements are also obtained against the stored energies in common with both plasmas.

The effect of Z_{eff} on the transport is examined in detail by using the limited plasma discharge with low electron density in which the highest ion temperature was obtained. The parameters used in the calculation are as follows; $\bar{n}_e=2.5\times10^{19}$ m^{-3}, $T_e(0)$=5.4 keV and P_{NB}^{inj}=18.8 MW. Profiles of the electron density and temperature determined by using the experimental data in the LOOK code are shown in Fig. 8. The profile index of electron density defined by the ratio, $n_e(0)/\bar{n}_e$, is 1.3-1.4 for the limited plasmas in the electron density region of 2.5-4$\times10^{19}$ m^{-3}, and is 1.2-1.25 for the diverted plasmas in the same region. The difference is not so large as to change the deposition profile of the neutral beam.

The Z_{eff}-dependence of ion temperature is shown in Fig. 9. In the calculation of the ion conduction loss, C_i=1 is used. As shown in Fig. 9, high ion temperatures around 10 keV are realized in case of $T_e(0)$=5.4 keV, irrespective of the value of Z_{eff}. In the experiment, the measured values of Z_{eff} are scattered between 4 and 7, but the effect of Z_{eff} on the determination of ion temperature seems week as long as high electron temperature is realized. From the calculation with constant electron confinement time, it is found that the increase in electron temperature with Z_{eff} is more effective to raise the ion temperature.

Figure 10 shows the total power flow of the neutral beam corresponding to the above calculation. With the increase in Z_{eff}, the total deposition power of neutral beam P_{abs}^{NB}, increases 30% due to the enhanced ionization rate by impurity ions. Since the critical beam energy, $E_{cr}=14.8T_e(n_{eff}/n_e)^{2/3}$ decreases from 67 keV at Z_{eff}=3 to 55 keV at Z_{eff}=6 with electron temperature of 5.4 keV, the power

deposition to the electron, P_{be}, increases about 50% at Z_{eff}=6, but the increase in power deposition to the ion, P_{bi}, is only 12%. Here, it should be noted that the power deposition per an ion, P_{bi}/n_{th}, increases with Z_{eff} because of decrease in number of thermal ions.

The ion temperature is determined in the ion power balance with the deposition power of P_{bi}. Figure 11 shows the ion power flow in the region of $r \leqq 1/2$. In this power flow, the dominant loss channel of ion energy are the convection loss and the equipartition loss. Since the particle flux, Γ, in the region of $r \leqq a/2$ increases with Z_{eff} due to the enhanced ionization by impurity ions, the convection loss tends to increase with Z_{eff}. On the other hand, the equipartition loss decreases with increase of Z_{eff} because the effective number of ions, n_{eff}, decreases. In the case that oxygen is a dominant impurity, n_{eff}/n_e becomes 0.7 at Z_{eff}=5. As a result, in case of constant electron temperature, T_e=5.4 keV, the change of ion temperature is small as shown in Fig. 8, although the deposition power per an ion increases. On the other hand, in case of constant electron confinement time, high electron temperatures are obtained because of increase in deposition power to the electron with Z_{eff}, which results in the decrease in equipartition loss with increase of Z_{eff}. Consequently, higher ion temperatures are obtained in the plasma with high Z_{eff}, provided the electron confinement time does not decrease with increase of Z_{eff}. From this analysis, it is considered that the difference in ion temperature between the limited and the diverted plasmas is mainly caused by the difference in electron temperature, which is caused by the increase in power deposition to electron with Z_{eff}.

Figure 12 shows the power deposition to the ions and the electrons in the region of $r \leqq a/2$ for the limited and the diverted plasmas. They are calculated with Z_{eff}=6 for the limited plasmas and with Z_{eff}=1.5 for the diverted plasmas. It is found that the power deposition to the electrons, $P_{be}(a/2)$, of the limited plasmas are larger by 30-50% than those of the diverted plasmas. The injection power of the neutral beam is 19-22 MW for the limited plasmas, and is 17-20 MW for the diverted plasmas. The difference in power deposition to the electron is caused by both the enhanced ionization by impurity ions and the decrease of the critical beam energy as described above. As shown in Fig. 13, the electron confinement times defined at $r \leqq 2a/3$,

$\tau_{Ee}=W_e/(P_{be}+P_{ie}+P_{joule})|_{r\leq 2a/3}$, are 45-55 msec for both plasmas in the electron density of $2.5\text{-}4\times10^{19}$ m^{-3}. There is no significant difference in electron confinement time between them. It is, hence, found that higher electron temperatures are sustained by the larger power deposition to the electrons which increases with Z_{eff}.

Figure 14 shows the Z_{eff}-dependence of the stored energies of the plasmas with low electron density corresponding to the calculation shown in Fig. 9. Because of the decrease in the number of thermal ions, the thermal ion stored energy decreases with Z_{eff}. Instead, the beam stored energy increases with increases in Z_{eff} and electron temperature, which results in the large total stored energy of the plasma with high Z_{eff}. In the case of low electron density plasmas, in fact, the beam energy becomes 50% of the total stored energy at $Z_{eff}=6$. It is, hence, considered that the stored energy, W*, of the 1 MA limited plasmas with low electron density is larger than those of the 1 MA diverted plasmas because of the enhanced increase in beam stored energy with Z_{eff}. This tendency does not change in the higher electron density region of 4×10^{19} m^{-3} although it becomes week. However, the stored energies of the 2 MA limited plasmas with electron density of 4×10^{19} m^{-3} is smaller than those of the diverted plasmas. This comes from the broad electron density and temperature profiles in the diverted plasmas, which results in the larger electron stored energy for the diverted plasmas with higher electron density.

6. Discussions and conclusion

The power deposition to ions, P_{bi}, used in the calculation of ion power balance in the SCOOP code is calculated with effective ion number for ionization $n_p + Z^{1.4}n_z$, in the OFMC code, where $n_p=n_{th}+n_f$. While, since the number of thermal ions, n_{th}, is used in the ion power balance, the deposition power to ions, P_{bi}, is thought to be overestimated, and to yield the high ion temperature of 10.5 keV at $Z_{eff}=6$ in the low electron density region. In the same calculation with the total proton number, $n_p=n_{th}+n_f$, ion temperature of 9.3 keV is obtained at $Z_{eff}=6$, but is thought to be underestimated. The reasonable value is thought to be between them. The difference is not

$\tau_{Ee}=W_e/(P_{be}+P_{ie}+P_{joule})|_{r\leq 2a/3}$, are 45-55 msec for both plasmas in the electron density of $2.5\sim4\times10^{19}$ m^{-3}. There is no significant difference in electron confinement time between them. It is, hence, found that higher electron temperatures are sustained by the larger power deposition to the electrons which increases with Z_{eff}.

Figure 14 shows the Z_{eff}-dependence of the stored energies of the plasmas with low electron density corresponding to the calculation shown in Fig. 9. Because of the decrease in the number of thermal ions, the thermal ion stored energy decreases with Z_{eff}. Instead, the beam stored energy increases with increases in Z_{eff} and electron temperature, which results in the large total stored energy of the plasma with high Z_{eff}. In the case of low electron density plasmas, in fact, the beam energy becomes 50% of the total stored energy at $Z_{eff}=6$. It is, hence, considered that the stored energy, W*, of the 1 MA limited plasmas with low electron density is larger than those of the 1 MA diverted plasmas because of the enhanced increase in beam stored energy with Z_{eff}. This tendency does not change in the higher electron density region of 4×10^{19} m^{-3} although it becomes week. However, the stored energies of the 2 MA limited plasmas with electron density of 4×10^{19} m^{-3} is smaller than those of the diverted plasmas. This comes from the broad electron density and temperature profiles in the diverted plasmas, which results in the larger electron stored energy for the diverted plasmas with higher electron density.

6. Discussions and conclusion

The power deposition to ions, P_{bi}, used in the calculation of ion power balance in the SCOOP code is calculated with effective ion number for ionization $n_p + Z^{1.4}n_z$, in the OFMC code, where $n_p=n_{th}+n_f$. While, since the number of thermal ions, n_{th}, is used in the ion power balance, the deposition power to ions, P_{bi}, is thought to be overestimated, and to yield the high ion temperature of 10.5 keV at $Z_{eff}=6$ in the low electron density region. In the same calculation with the total proton number, $n_p=n_{th}+n_f$, ion temperature of 9.3 keV is obtained at $Z_{eff}=6$, but is thought to be underestimated. The reasonable value is thought to be between them. The difference is not

so large to change the results of the transport analysis on the Z_{eff}-dependence of ion temperature described above.

The Z_{eff}-dependences of ion temperature etc. described above are calculated taking account of the effect of oxygen ions plus titanium ions of 0.3 %. As the extreme case, by taking titanium ions as dominant impurities without oxygen ions, the effect of metal impurity on the transport is compared with the above results. In this case, the power deposition to electron, P_{be}, is small (4.5 MW at Z_{eff}=6) compared with the above case (6.2 MW at Z_{eff}=6), which is due to both the increase in charge exchange loss and the week Z_{eff}-dependence of the critical beam energy. In the case of titanium ions, the charge exchange loss becomes 5 MW at Z_{eff}=6 because of increase in the number of proton (n_p/n_e=0.76), and the critical beam energy stays at E_{cr}=67 keV against E_{cr}=55 keV in the case of oxygen ions. As a result, the electron energy confinement time defined at $r \leqq 2/3a$ becomes 70 msec. Taking account of the large radiation loss observed in the experiment, it is not likely that this value is actually realized. It is, hence, considered to be light impurities rather than heavy impurities that are effective to raising ion and electron temperatures.

In conclusion, the attainment of high ion temperatures in the neutral beam heating of the limited plasmas is found to be due to the effect of high Z_{eff} contributed by light impurity, oxygen. With increase in Z_{eff}, the deposition power to electron increases and sustains the electron temperature higher, which is considered to be the "key" of the attainment of high ion temperature. In addition to decrease in the effective number of ions, n_{eff}, with increase in Z_{eff}, the high electron temperature reduces the equipartition loss of ion energy which is dominant in the ion power balance. Consequently, the high ion temperature is obtained in the limited plasmas with high Z_{eff}.

In JT-60, the experiments have been mainly performed with hydrogen gas ($H^0 \rightarrow H^+$). It is generally considered that the energy confinement time of hydrogen plasma is smaller than that of deutrium plasma by about the square root of their mass ratio [10]. Hence, according to the analysis described here, it is considered difficult to obtain high ion temperature of order of 10 keV in the diverted plasmas with low Z_{eff} like JT-60 without any improvement in energy confinement. However, with deutrium gas, it is considered possible to

attain high ion temperature above 10 keV in JT-60 like the other large tokamaks.

Acknowledgement

The authors would like to thank Drs. A. Tomabechi and M. Yoshikawa for their encouragements on this work.

References

[1] THE JET TEAM, in Plasma Physics and Controlled Nuclear Fusion Research (Proc. 11th Int. Conf. Kyoto, 1986)

[2] HAWRYLUK, R.J., et al., in Plasma Physics and Controlled Nuclear Fusion Research (Proc. 11th Inc. Conf. Kyoto, 1986)

[3] YOSHIKAWA, M., et al., in Plasma Physics and Controlled Nuclear Fusion Research (Proc. 11th Int. Conf. Kyoto, 1986)

[4] JT-60 TEAM presented by NAGAMI, M., in Plasma Physics and Controlled Nuclear Research (Proc. 11th Int. Conf. Kyoto, 1986)

[5] HIRAYAMA, T., SHIMIZU, K., TANI, K., KIKUCHI, M., et al., "Experimental Transport Analysis System in JT-60", to be published in JAERI-M.

[6] TANI, K., AZUMI, M., OHTSUKA, M., KISHIMOTO, H., TAMURA, S., in Heating in Toroidal Plasma (Proc. Joint Varenna-Grenoble Int. Symp. 1978), vol. 1 (1978) 31.

[7] OLSON, R.E., SALOP, A., Stanford Research Institute Annual Report (1977).

[8] NAKAI, Y., et al., KAKUYUGO KENKYU, 39 (1978) 241.

[9] CHANG, C.S. and HINTON, F.L., Phys. Fluids 25 (1982) 1493.

[10] SHIMOMURA, Y., SUZUKI, N., SUGIHARA, M., TSUDA, T., ODAJIMA, K. and TSUNEMATSU, T., JAERI-M 87-080 (1987)

attain high ion temperature above 10 keV in JT-60 like the other large tokamaks.

Acknowledgement

The authors would like to thank Drs. A. Tomabechi and M. Yoshikawa for their encouragements on this work.

References

[1] THE JET TEAM, in Plasma Physics and Controlled Nuclear Fusion Research (Proc. 11th Int. Conf. Kyoto, 1986)

[2] HAWRYLUK, R.J., et al., in Plasma Physics and Controlled Nuclear Fusion Research (Proc. 11th Inc. Conf. Kyoto, 1986)

[3] YOSHIKAWA, M., et al., in Plasma Physics and Controlled Nuclear Fusion Research (Proc. 11th Int. Conf. Kyoto, 1986)

[4] JT-60 TEAM presented by NAGAMI, M., in Plasma Physics and Controlled Nuclear Research (Proc. 11th Int. Conf. Kyoto, 1986)

[5] HIRAYAMA, T., SHIMIZU, K., TANI, K., KIKUCHI, M., et al., "Experimental Transport Analysis System in JT-60", to be published in JAERI-M.

[6] TANI, K., AZUMI, M., OHTSUKA, M., KISHIMOTO, H., TAMURA, S., in Heating in Toroidal Plasma (Proc. Joint Varenna-Grenoble Int. Symp. 1978), vol. 1 (1978) 31.

[7] OLSON, R.E., SALOP, A., Stanford Research Institute Annual Report (1977).

[8] NAKAI, Y., et al., KAKUYUGO KENKYU, 39 (1978) 241.

[9] CHANG, C.S. and HINTON, F.L., Phys. Fluids 25 (1982) 1493.

[10] SHIMOMURA, Y., SUZUKI, N., SUGIHARA, M., TSUDA, T., ODAJIMA, K. and TSUNEMATSU, T., JAERI-M 87-080 (1987)

attain high ion temperature above 10 keV in JT-60 like the other large tokamaks.

Acknowledgement

The authors would like to thank Drs. A. Tomabechi and M. Yoshikawa for their encouragements on this work.

References

[1] THE JET TEAM, in Plasma Physics and Controlled Nuclear Fusion Research (Proc. 11th Int. Conf. Kyoto, 1986)

[2] HAWRYLUK, R.J., et al., in Plasma Physics and Controlled Nuclear Fusion Research (Proc. 11th Inc. Conf. Kyoto, 1986)

[3] YOSHIKAWA, M., et al., in Plasma Physics and Controlled Nuclear Fusion Research (Proc. 11th Int. Conf. Kyoto, 1986)

[4] JT-60 TEAM presented by NAGAMI, M., in Plasma Physics and Controlled Nuclear Research (Proc. 11th Int. Conf. Kyoto, 1986)

[5] HIRAYAMA, T., SHIMIZU, K., TANI, K., KIKUCHI, M., et al., "Experimental Transport Analysis System in JT-60", to be published in JAERI-M.

[6] TANI, K., AZUMI, M., OHTSUKA, M., KISHIMOTO, H., TAMURA, S., in Heating in Toroidal Plasma (Proc. Joint Varenna-Grenoble Int. Symp. 1978), vol. 1 (1978) 31.

[7] OLSON, R.E., SALOP, A., Stanford Research Institute Annual Report (1977).

[8] NAKAI, Y., et al., KAKUYUGO KENKYU, 39 (1978) 241.

[9] CHANG, C.S. and HINTON, F.L., Phys. Fluids 25 (1982) 1493.

[10] SHIMOMURA, Y., SUZUKI, N., SUGIHARA, M., TSUDA, T., ODAJIMA, K. and TSUNEMATSU, T., JAERI-M 87-080 (1987)

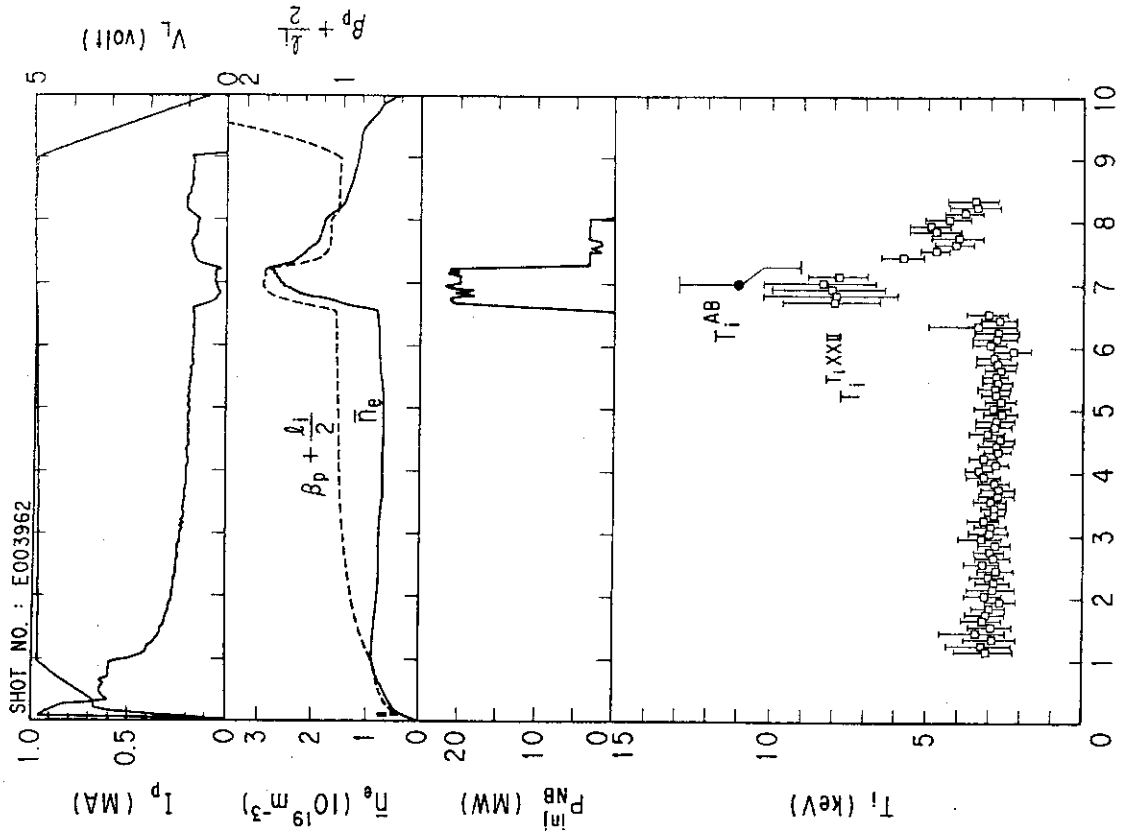

Fig. 2 Typical waveforms of the limiter discharge in which ion temperature of 11±2 keV was obtained.

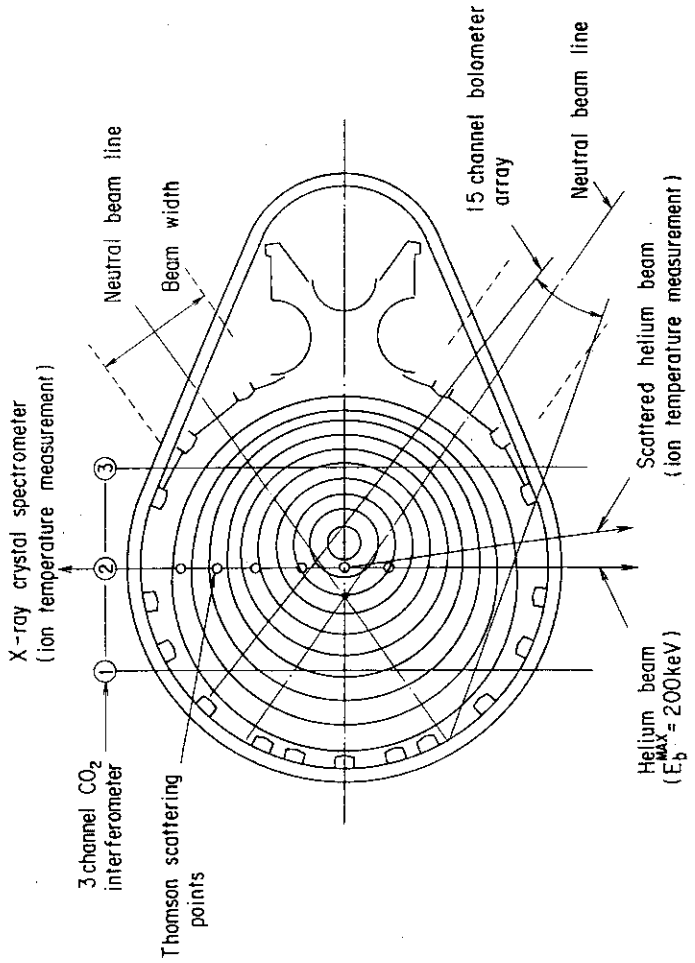

Fig. 1 The cross-sectional view of JT-60 and the arrangement of the "key" diagnostics in this experiment.

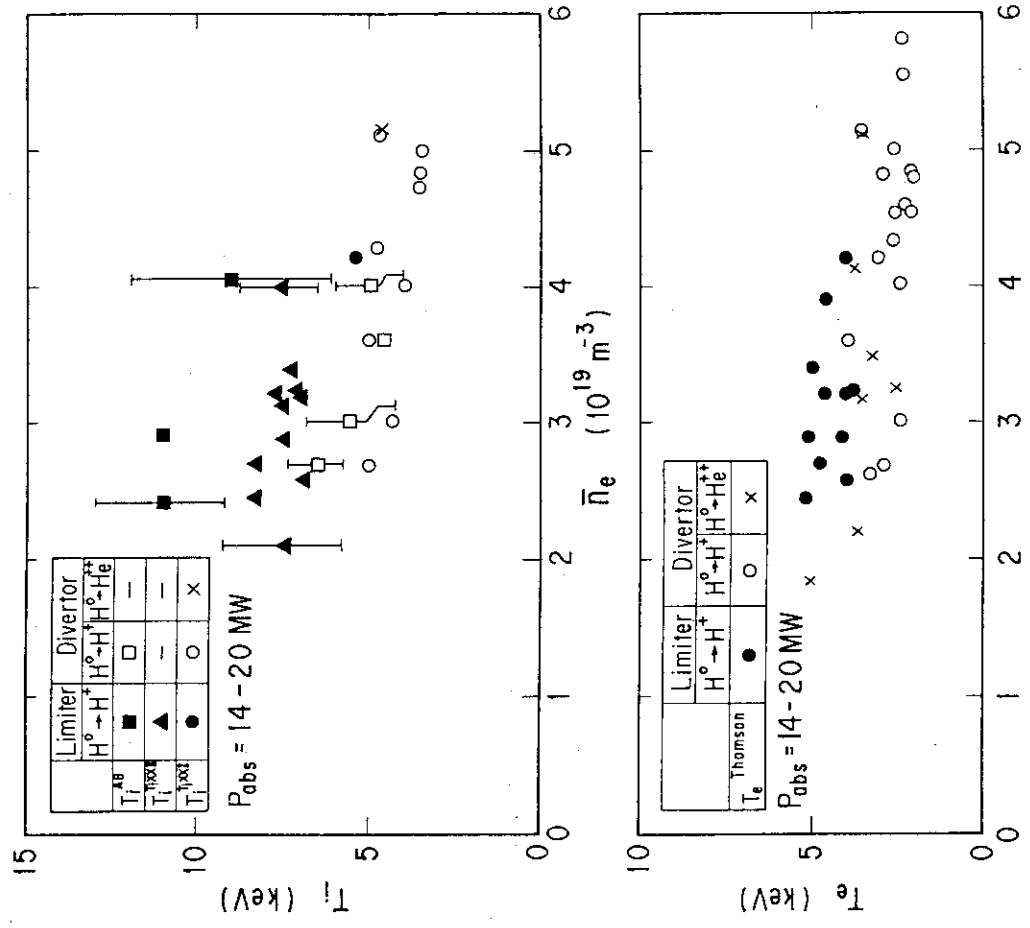

Fig. 4 Electron density dependences of ion and electron temperatures for the limited and diverted plasmas. T_i^{AB}, T_i^{TiXXI} and T_i^{TiXXII} are same as shown in Fig. 3.

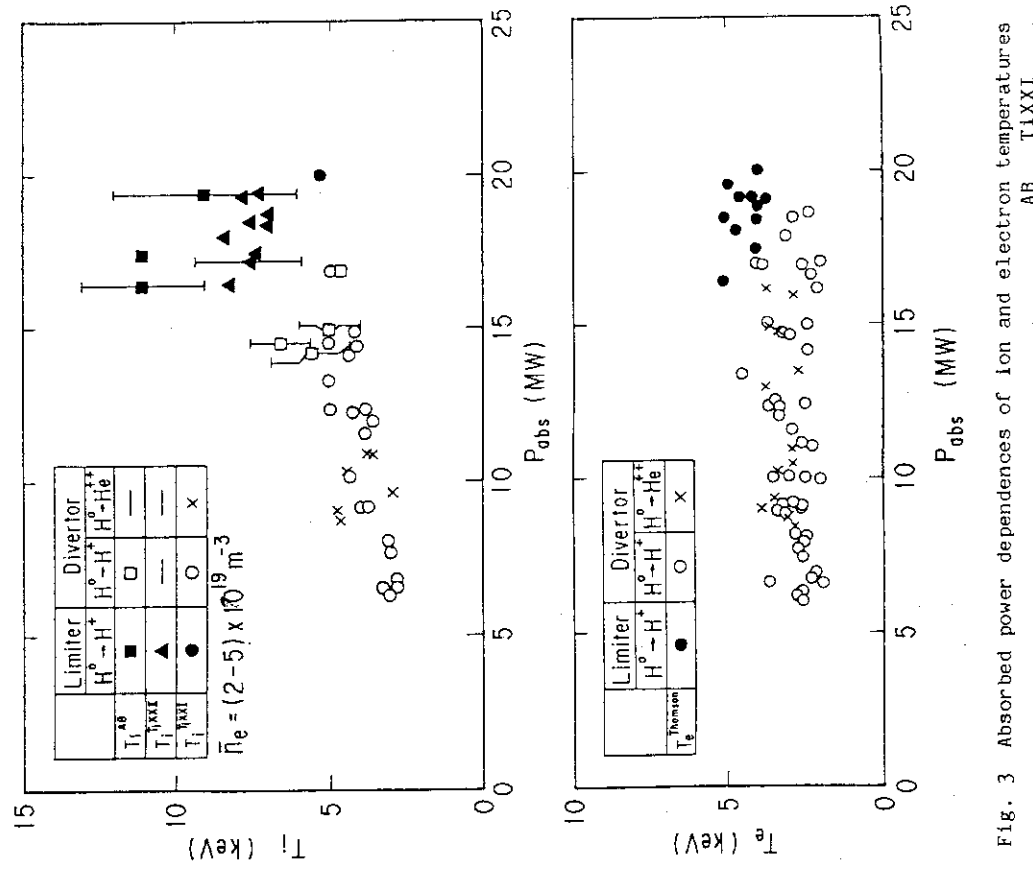

Fig. 3 Absorbed power dependences of ion and electron temperatures for the limited and the diverted plasmas. T_i^{AB}, T_i^{TiXXI} and T_i^{TiXXII} are ion temperatures measured by the forward scattering of helium beam with energy of 180－200 keV and the doppler broadening of titanium line emissions, TiXXI and TiXXII.

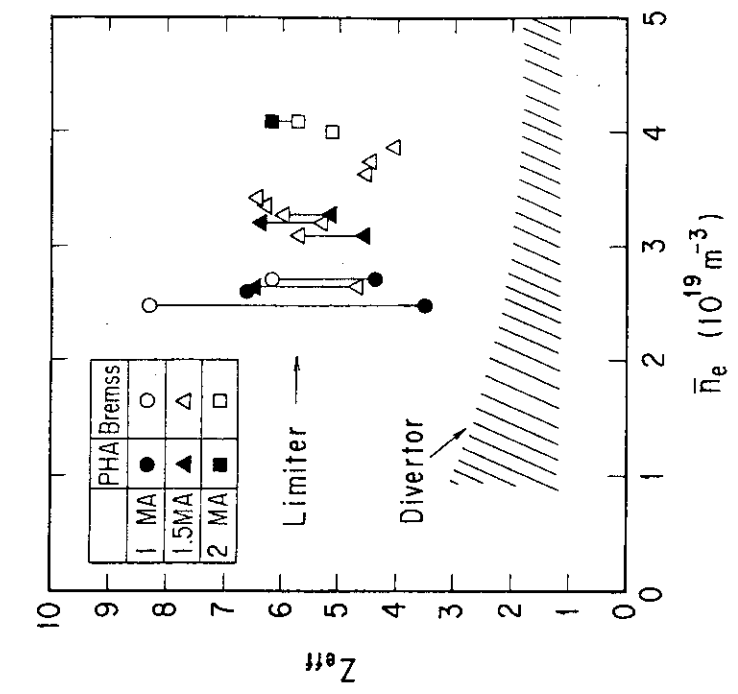

Fig. 6 Z_{eff} of the limited and the diverted plasmas during the neutral beam heating.

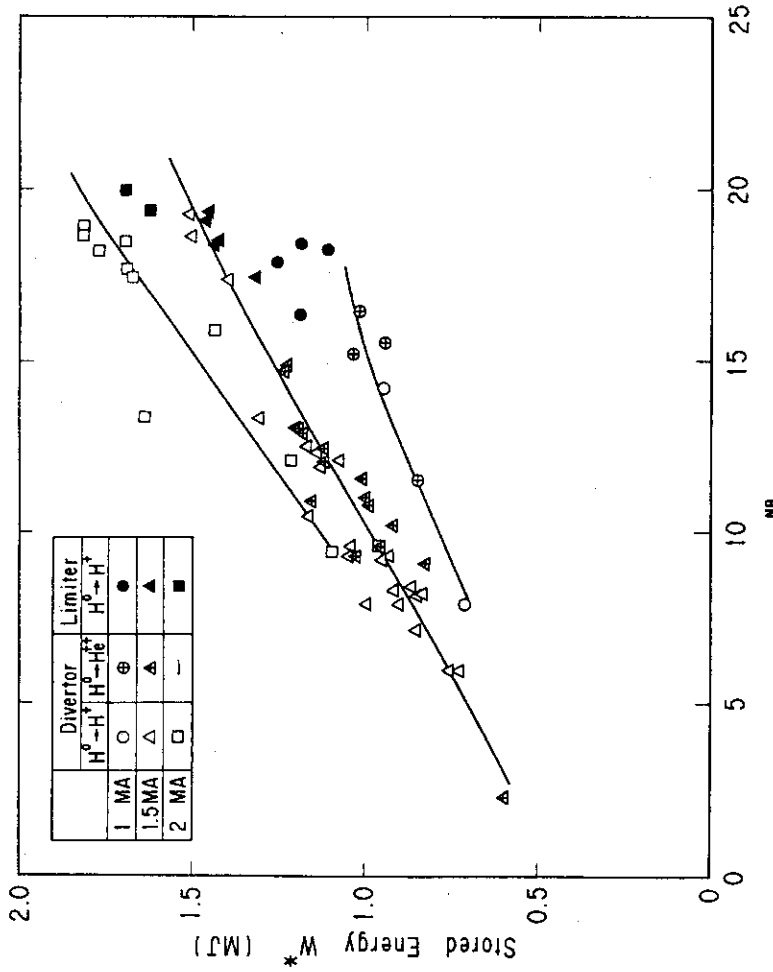

Fig. 5 Absorbed power dependences of stored energies for the limited and diverted plasmas.

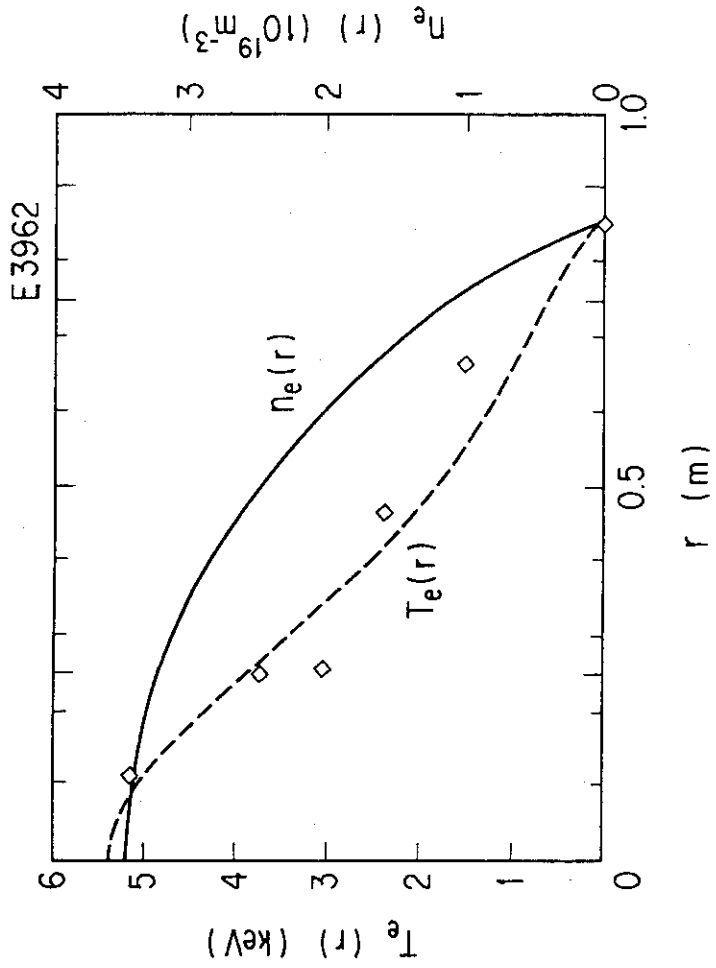

Fig. 8 Profiles of electron density and electron temperature of the limited plasma in which ion temperature of 11±2 keV was obtained.

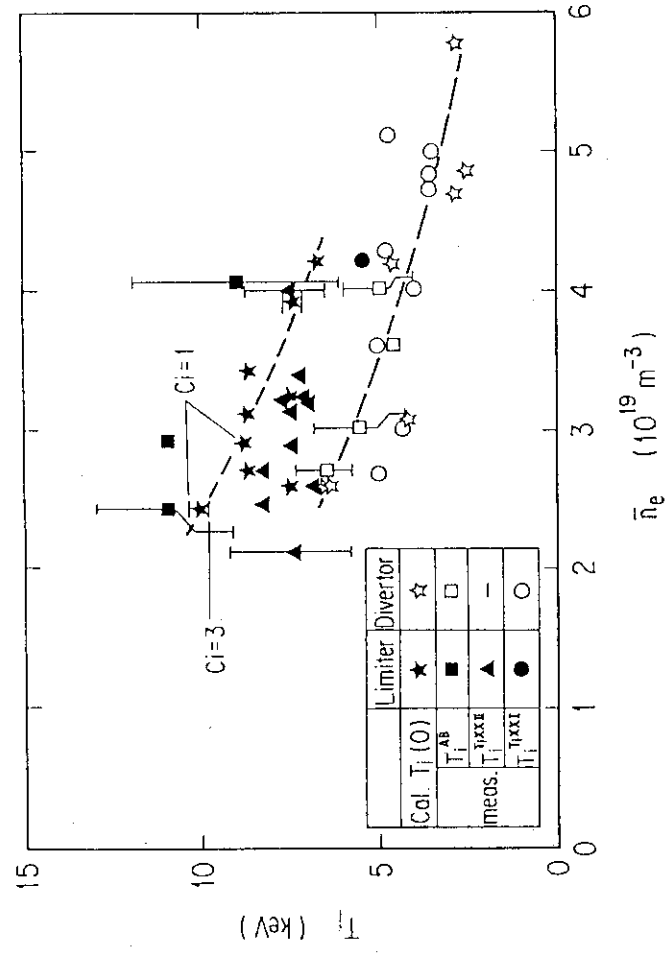

Fig. 7 Comparson of central ion temperatures calculated with the LOOK/OFMC/SCOOP code and measured ion temperatures. In the calculation, Z_{eff}=6 is used for the limited plasmas and Z_{eff}=1.5 for the diverted plasmas, and C_1=1 is used for both plasmas.

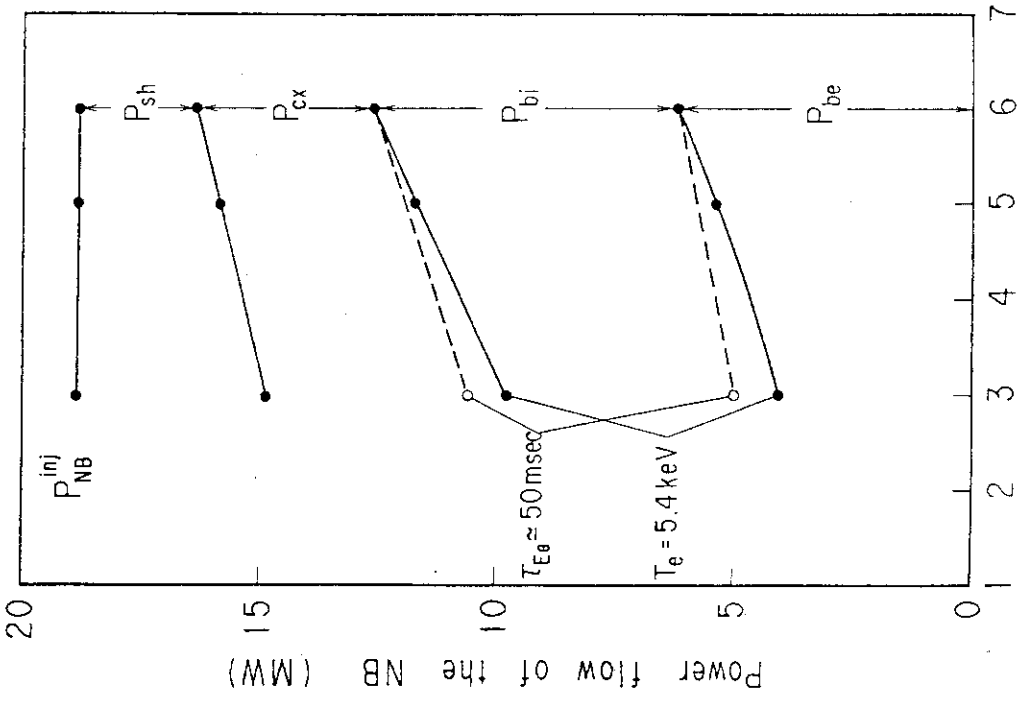

Fig. 10 Z_{eff}-dependence of the power flow of neutral beam. The calcuation condition is same as shown in Fig. 10. P_{be}: power deposition to electron, P_{bi}: power deposition to ions, P_{cx}: charge exchange loss, P_{sh}: shine-through loss. Here, the deposition power to impurity ion is included in P_{bi}.

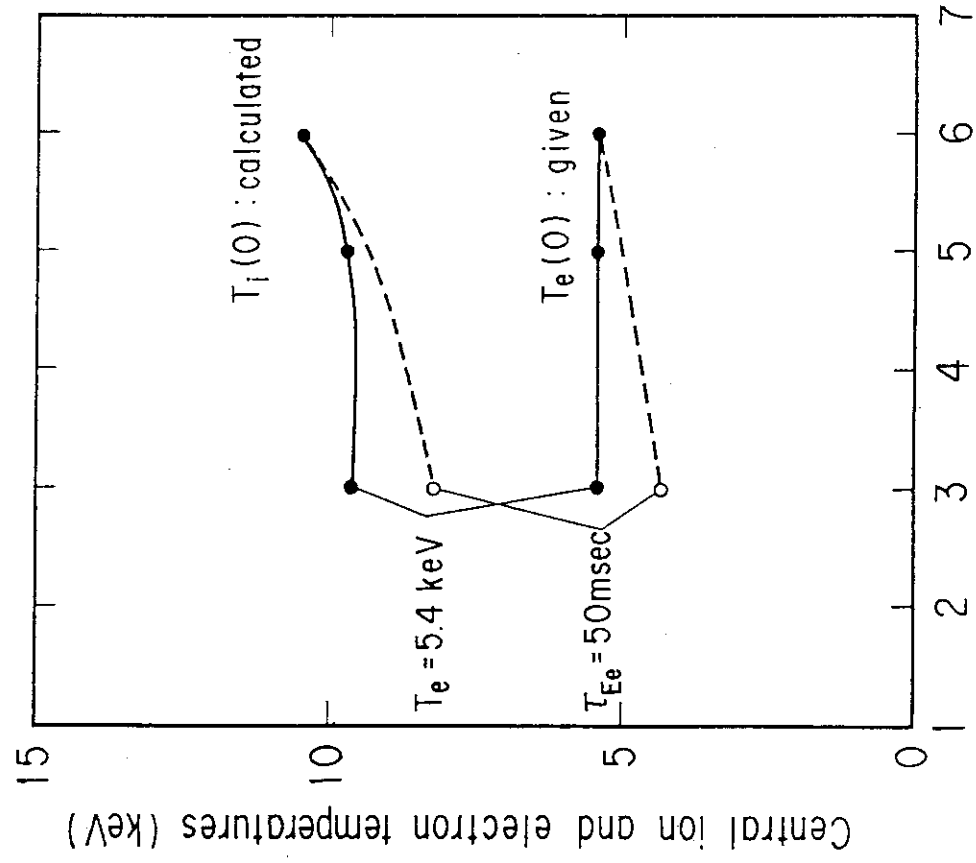

Fig. 9 Z_{eff}-dependence of ion temperature. The calculation condition is as follows; $\bar{n}_e = 2.5 \times 10^{19}$ m^{-3}, $P_{NB}^{inj} = 18.8$ MW. $\tau_p = 20$ msec and $C_I = 1$. The same profiles of electron temperature and density as E3962 are used.

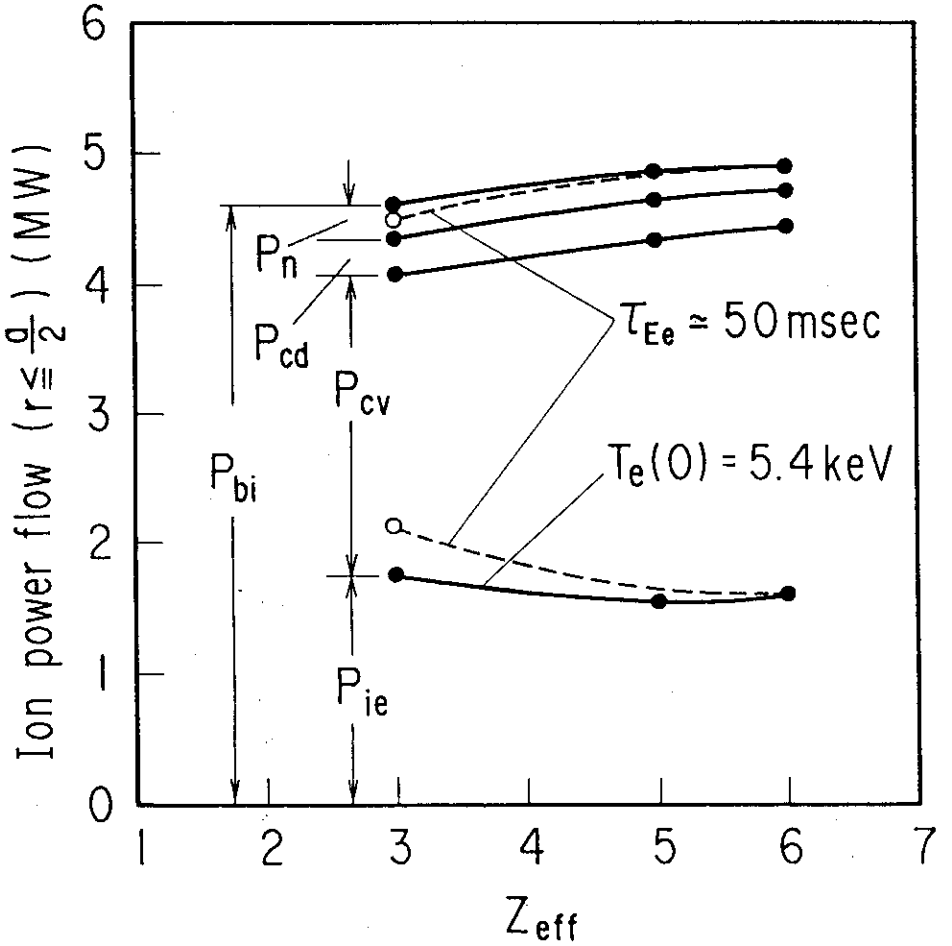

Fig. 11 Z_{eff}-dependence of ion power flow at r=a/2 corresponding to the calculations shown in Figs. 9 and 10. P_{bi}: power deposition to ions, P_{ie}: equipartition loss, P_{cv}: convection loss, P_{cd}: conduction loss, P_n: charge exchange loss of thermal ions. C_i is used in the calculation of P_{cd}.

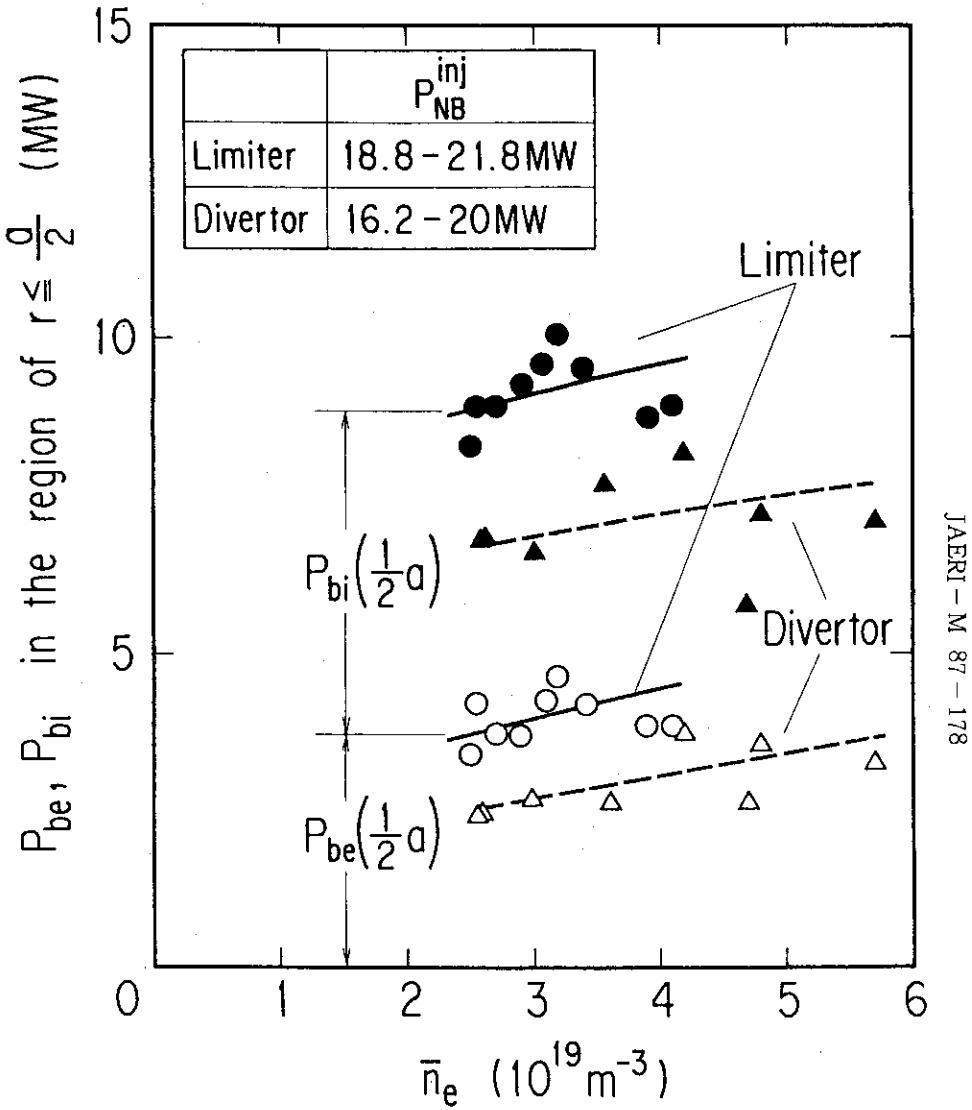

Fig. 12 Comparison of power deposition to ion and electron in the region of r≦a/2 for the limited and the diverted plasmas.

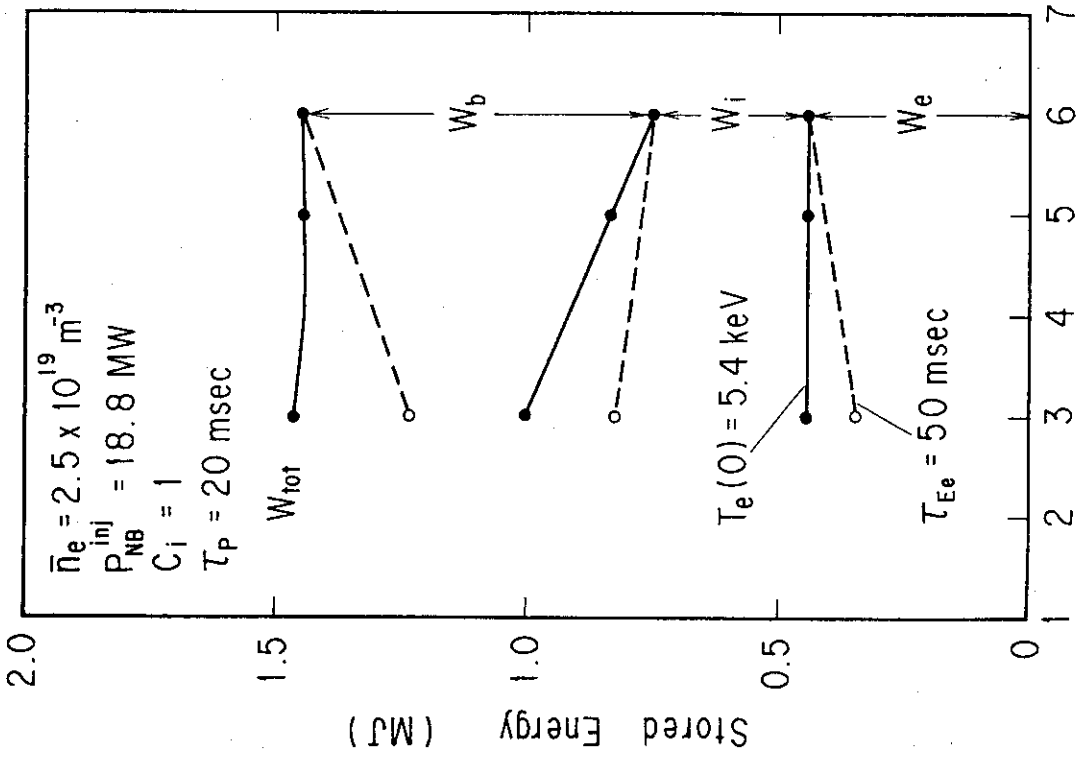

Fig. 14 Z_{eff}-dependence of stored energy of low electron density plasma corresponding to the calculation shown in Fig. 9.

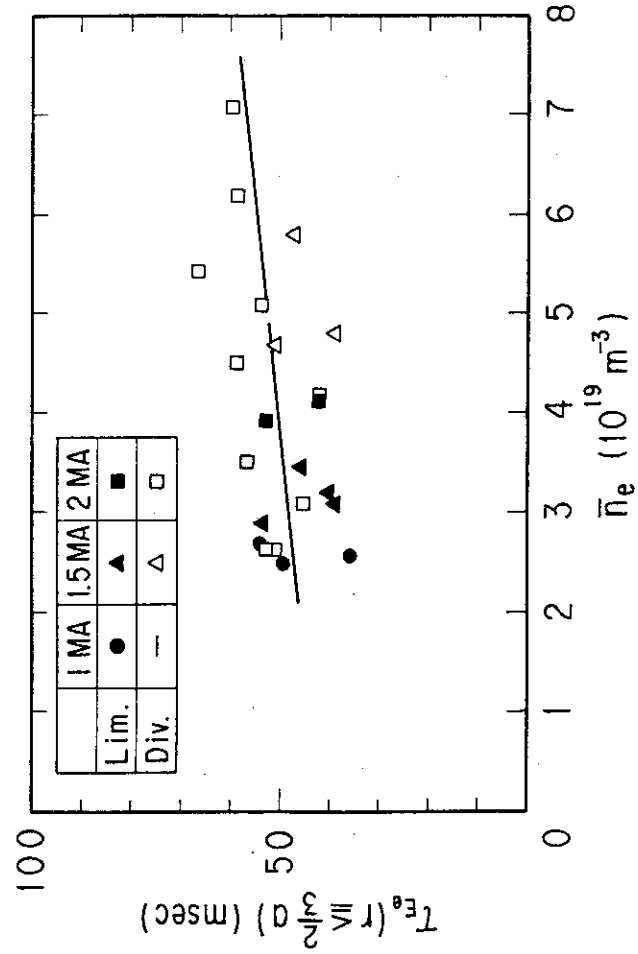

Fig. 13 Electron energy confinement time defined at r≤2/3a for the limited and the diverted plasmas.